Emanation Graph: A New t-Spanner[*]

Bardia Hamedmohseni[†]   Zahed Rahmati[‡]   Debajyoti Mondal[§]

Abstract

We introduce a new *t-spanner*, called *emanation graph* M_k, based on the idea of shooting rays out of each vertex at specific angles, determined by k, the *grade* of the emanation graph. Emanation graphs of grade one coincide with the competition mesh, which was studied by Mondal and Nachmanson [18] in the context of network visualization. They proved that the spanning ratio of such a graph is bounded by $(2 + \sqrt{2}) \approx 3.41$.

In this paper, we prove an improved $\sqrt{10} \approx 3.162$ upper bound on the spanning ratio of emanation graphs of grade one, which in fact improves the previous result. We also prove that the spanning ratio of the emanation graphs of grade k is at least $\frac{2+\sin(\frac{\pi}{2^k})}{1+\cos(\frac{\pi}{2^k})}$, for sufficiently large n.

1 Introduction

Let G be a geometric graph embedded in the Euclidean plane, and let u and v be a pair of vertices in G. Let $d_G(u,v)$ and $d_E(u,v)$ be the minimum graph distance (i.e., shortest path distance) and Euclidean distance between u and v, respectively. The *spanning ratio* of G is $\max_{\{u,v\}\in G} \frac{d_G(u,v)}{d_E(u,v)}$, i.e., the maximum ratio between $d_G(u,v)$ and $d_E(u,v)$ over all pairs of vertices $\{u,v\}$ in G. Graph G is called a *t-spanner* of the complete geometric graph, if for every pair of vertices $\{u,v\}$ in G, the distance $d_G(u,v)$ is at most t times of their Euclidean distance $d_E(u,v)$.

The *t-spanners* are commonly used in computational geometry. They also find applications in wireless network routing [9] and in network visualizations [18, 19]. A rich body of research is devoted towards the construction of *t*-spanners, and there has also been significant efforts to find tight spanning ratios for different classes of geometric graphs.

In this paper, we examine *plane geometric spanners*, i.e., no two edges in the spanner cross except at their

---

[†]Department of Mathematics and Computer Science, Amirkabir University of Technology, Tehran, Iran `hamedmohseni@aut.ac.ir`

[‡]Department of Mathematics and Computer Science, Amirkabir University of Technology, Tehran, Iran `zrahmati@aut.ac.ir`

[§]Department of Computer Science, University of Saskatchewan, Saskatoon, Canada `dmondal@cs.usask.ca`
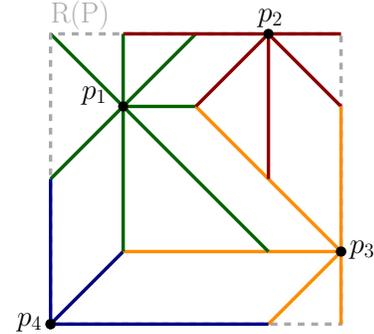

Figure 1: The emanation graph of grade two, for four points in the Euclidean plane.

common endpoints. A natural question in this context is as follows: Given a set of points P of n points in the plane, can we compute a planar spanner $G = (V, E)$ of P with small size, degree and spanning ratio? We allow the spanner to have Steiner points, i.e., $P \subseteq V$, thus V may contain vertices that do not correspond to any point of P. Note that keeping the degree, size and spanning ratio of the spanners small are often motivated by application areas, and appeared in the literature [9, 8]. Note that we do not require the paths between a pair of Steiner points to be bounded.

In this paper, we introduce a new type of *t-spanners*, called the *emanation graph*. Given a set P of n points in a bounding box $R(P)$, and an integer $k > 0$, the *emanation graph M_k of grade k* is constructed by emanating, from each point $p_i \in P$, 2^{k+1} rays with equal angular distances of $\frac{\pi}{2^k}$, and equal constant speed. Each ray stops as soon as it hits another ray of larger length, or $R(P)$. If two parallel rays collide, then they both stop and if two or more non-parallel rays of equal length collide, then arbitrarily one of them continues, and the other rays stop. The vertices formed by the collision of rays are considered as Steiner points. Figure 1 depicts M_2 for four points in the plane.

In the following we briefly review the literature related to the planar spanners (both with and without Steiner points).

1.1 Background

Delaunay graphs are one of the most studied plane geometric spanners. Chew [10] showed that the L_1-metric Delaunay graph is a $\sqrt{10}$-spanner. There have been sev-

eral attempts to find tight spanning ratio for Delaunay triangulations (L_2-metric Delaunay graphs) [16, 12, 6]. The currently best known upper and lower bound on the spanning ratio of the Delaunay triangulation is 1.998 [20] and 1.5932 [21], respectively.

Another popular class of plane geometric spanner is *half-Θ_6 graphs*, which is formed by partitioning the space around each vertex into six cones of equal angle, and then connecting the vertex to the bisector nearest neighbor in the first, third and fifth cones (for some fixed clockwise ordering of the cones); the bisector nearest neighbor in a cone means the neighbor with the smallest projection on the bisector of the cone. The half-Θ_6 graphs are 2-spanners [10].

While both the Delaunay triangulations and half-Θ_6 graphs have linear number of edges and small spanning ratio, they may have vertices with *unbounded* degree. Bose et al. [7] showed that plane t-spanners of bounded degree exist (for some constant t). A significant amount of research followed this result, which examines the construction of bounded degree plane spanners with low spanning ratio. Some of the best known spanning ratios for spanners with maximum degree $4, 6$ and 8 are 20 [15], 6 [4] and 4.414 [8], respectively.

Although there exist point sets that do not admit a planar spanner of spanning ratio less than 1.43 [13], by allowing $O(n)$ Steiner points, one can obtain a spanning ratio of $(1+\epsilon)$-spanners, for any $\epsilon > 0$. Arikati et al. [1] showed that one can construct a plane geometric $(1+\epsilon)$-spanner with $O(n/\epsilon^4)$ Steiner points. Bose and Smid [9] asked whether the dependence on ϵ can be improved.

Recently, Dehkordi et al. [11] proved that any set of n points admits a 'planar angle-monotone graph of width 90°' with $O(n)$ Steiner points. Since an angle mono-tone graphs of width α is a $\frac{1}{\cos(\alpha/2)}$-spanner [3], this implies the existence of a $\sqrt{2}$-spanner with $O(n)$ Steiner points, which may contain vertices of *unbounded* degree. See [17] for more details on the construction of angle-monotone graphs with Steiner points.

Mondal and Nachmanson introduced a class of geometric graphs (with Steiner points), called *competition mesh*, and used those graphs to implement a large network visualization system (GraphMaps [18]). They proved the competition mesh is a $(2 + \sqrt{2})$-spanner. A competition mesh is exactly the emanation graph of grade one, and hence their result implies an upper bound of $(2+\sqrt{2})$ on the spanning ratio of M_1. Mondal and Nachmanson [18] noticed that the competition mesh can be viewed as a variation of a motorcycle graphs [14]. This also holds for the emanation graphs.

Instead of choosing three cones in the half-Θ_6 graphs, one can connect a vertex to the bisector nearest neighbors in all the six cones, which gives rise to the full-Θ_6 graphs. The concept has also been extended to full-Θ_r graphs [5], where the space around the vertices
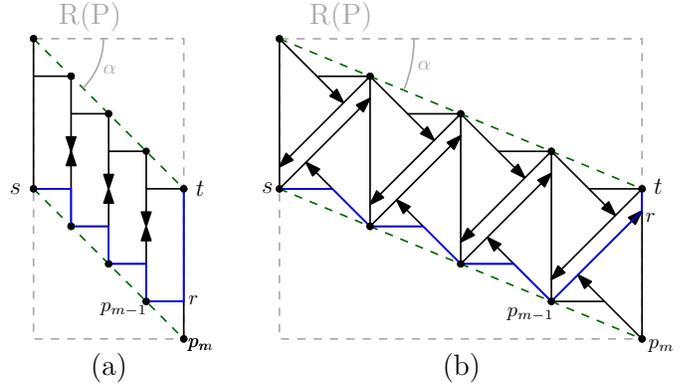

Figure 2: Illustration for lower bound proof.

are partitioned into r cones of equal angle $\theta = 2\pi/r$. Similarly, there exist Yao-graphs Y_r, where the nearest neighbor in a cone is chosen based on the Euclidean distance [2]. However, all these generalizations yield *non-planar* spanners.

1.2 Contributions

We introduce a class of *plane* geometric spanners, called emanation graphs, which generalizes the competition mesh [18]. We prove a $\sqrt{10}$ upper bound on the spanning ratio of emanation graphs of grade one, which improves the previously known upper bound of $(2 + \sqrt{2})$. We also prove that the spanning ratio of every emanation graph with r rays, where $r = 4q+2$ and $q \geq 1$, is at most $\frac{1}{\sin(\pi/r)\sin(\pi/2r)}$. In contrast, we prove the spanning ratio of the emanation graphs of grade k to be at least $\frac{2+\sin(\frac{\pi}{2^k})}{1+\cos(\frac{\pi}{2^k})}$ (for sufficiently large n). Note that Mondal and Nachmanson [18] proposed several heuristics to simplify the emanation graphs (e.g., deleting the segments that do not lie on the shortest paths), which can also be applied to emanation graphs of higher grade. However, we do not consider any such simplification methods in this paper.

2 Lower Bounds

In this section, we prove the lower bounds on the spanning ratio of the emanation graphs.

Theorem 1 *There exists an emanation graph M_k of n vertices with spanning ratio $\frac{2+\sin(\frac{\pi}{2^k})}{1+\cos(\frac{\pi}{2^k})}$, for sufficiently large n.*

Proof. We refer the reader to Figures 2(a) and (b), which depict the case when $k = 1$ and $k = 2$, respectively. We construct a set of n points inside a bounding box R as follows. Imagine two parallel guidelines with an angle of $\alpha = \frac{\pi}{2^{k+1}}$, as shown in green dashed
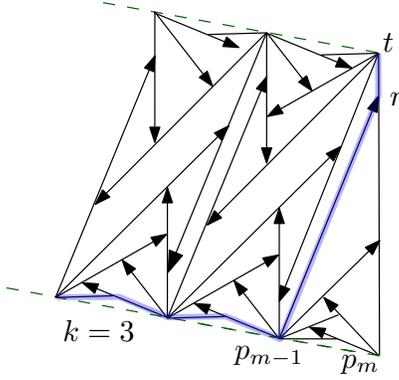
Figure 3: Illustration for the case when $k = 3$.

lines. Specifically, the two points s and t, which will achieve the lower bound, are lying along the horizontal axis. One of the two guidelines starts at s and the other guideline starts at t. As shown in the figure, the top-left corner of the bounding box R is determined by the intersection of the vertical line through s and the guideline that starts at t. The bottom-right corner of R is determined by the intersection of the vertical line through t and the guideline that starts at s.

We may assume that the number of vertices is even (if the number of vertices is odd, then we place one vertex on the bottom-left corner of R). We distribute $n/2$ points $p_1, p_2, \ldots, p_{n/2}(= p_m)$ on the guideline incident to s. We place the points ensuring that the segments $p_i p_{i+1}$ all have the same length. We place the rest of the points symmetrically on the other guideline.

We now define a canonical path $\mathcal{L}$ that starts at s and ends at t, as follows. The path $\mathcal{L}$ visits all the points $s(= p_1), \ldots, p_{m-1}$, by following the rays closest to the guidelines but staying above the guideline. The path continues from p_{m-1} by following the ray that reach closest to t. Assume that the ray intersects R at point r. Then the path continues the vertical segment rt to reach t. Figures 2(a) and (b) depict the path $\mathcal{L}$ in blue. Figures 3 illustrates the scenario when $k = 3$. We will later prove in Lemma 2 that the canonical path $\mathcal{L}$ is a shortest path between s and t.

For any two points a and b, we denote the horizontal and vertical distances between them by $|ab|_x$ and $|ab|_y$, respectively. By $\overline{ab}$, we denote the straight line segment connecting a and b. Note that s and t are horizontally aligned, and p_m is vertically aligned with t. Assume that $d_E(p_i, p_{i+1}) = 2$, and $d_E(p_1, p_m) = 2(m-1)$, where $m = n/2$. Therefore, $|p_m t|_y = 2(m-1)\sin\alpha$, and $|sp_m|_x = 2(m-1)\cos\alpha$ which is equal to $d_E(s, t)$.

Since the triangle $\triangle p_{m-1} p_m r$ is isosceles, the length of $\overline{p_{m-1}r}$ is equal to that of $\overline{p_m r}$. The length of the subpath $p_1, \ldots, p_{m-1}$ of $\mathcal{L}$ is $2(m-2)/\cos\alpha$, so the

graph distance $d_G(s, t)$ between s and t is

$$\frac{2(m-2)}{\cos\alpha} + |p_m t|_y = \frac{2(m-2)}{\cos\alpha} + 2(m-1)\sin\alpha.$$

Lemma 2 proves that the shortest path between s and t is $\mathcal{L}$. Thus the spanning ratio would be

$$\begin{aligned} \frac{d_G(s,t)}{d_E(s,t)} &= \frac{\frac{2(m-2)}{\cos\alpha} + 2(m-1)\sin\alpha}{2(m-1)\cos\alpha} \\ &= \frac{2(m-2) + 2(m-1)\cos\alpha\sin\alpha}{2(m-1)\cos^2\alpha} \end{aligned}$$

For a sufficiently large m, the proof obtains:

$$\begin{aligned} \lim_{m\to\infty} \frac{d_G(s,t)}{d_E(s,t)} &= \frac{2 + 2\cos\alpha\sin\alpha}{2\cos^2\alpha} \\ &= \frac{2 + \sin(2\alpha)}{1 + \cos(2\alpha)} \\ &= \frac{2 + \sin(\frac{\pi}{2^k})}{1 + \cos(\frac{\pi}{2^k})}. \end{aligned}$$

$\square$

Theorem 1 concludes that the lower bound of spanning ratio for the emanation graph of grade $k = 1$ is 3, and for a graph of grade $k = 2$ is approximately 1.58.

Lemma 2 *The selected path in Theorem 1 is a shortest path between s and t.*

Proof. (Sketch) We use the construction described in Theorem 1 (e.g., see Figure 4) to show that any path from s to t is at least as large as the canonical path $\mathcal{L}$ (marked in blue). First observe that it suffices to restrict our attention to x-monotone paths. One can categorize the candidate monotone paths in two groups: (I) Paths that have the same length as $\mathcal{L}$, such paths can be formed by replacing segments of $\mathcal{L}$ by their symmetric counterparts, two of these counterparts are highlighted in yellow. (II) Paths with segments that do not belong to (I), two of such segments are highlighted in red. We only need to show that the paths in (II) can not be shorter than that of $\mathcal{L}$.

By the symmetric structure of the graph, it is straightforward to observe that the paths in (II) can gradually be transformed into the canonical path $\mathcal{L}$ without changing the length. For example, the yellow path from p_j to t can be replaced by the blue path from p_j to t. Appendix includes the formal details. $\square$

3 Upper Bounds

In this section we give the upper bounds on the spanning ratio of the emanation graphs.
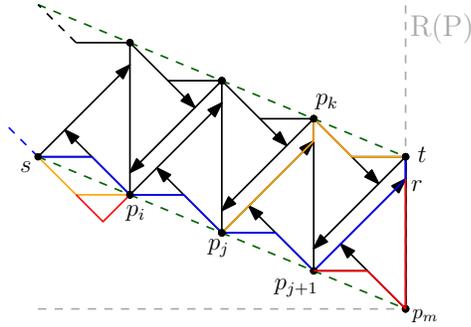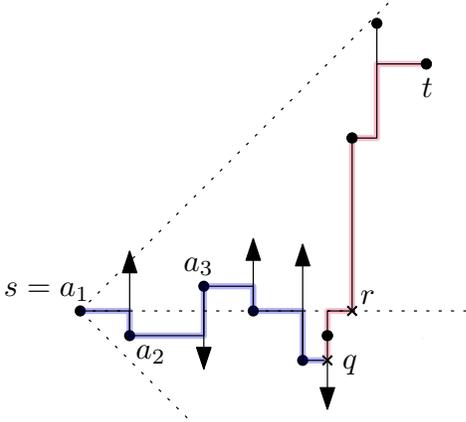
Figure 4: Illustration for proof of Lemma 2.

Figure 5: Illustration for proof of Theorem 3.

3.1 Emanation Graphs of Grade One

Theorem 3 *The spanning ratio of every emanation graph of grade one is at most* $\sqrt{10} \approx 3.162$.

Proof. Let s and t be a pair of vertices in the emanation graph. Consider four cones around s, where the cones are determined by two lines passing through s with slopes $+1$ and -1, respectively, as illustrated in Figure 5. Without loss of generality assume that t lies in the rightward cone C of s.

We now construct an x-monotone path P_x, which lies entirely in cone C, as follows: The path starts at s and for each original vertex, the path follows its rightward segment ℓ. If a rightward segment is stopped by another segment ℓ', then the path follows ℓ' to the original vertex that created ℓ'. Figure 5 illustrates a subpath $s(= a_1), \ldots, q$ of P_x in blue. For any subpath $a_i, \ldots, a_j$ on P_x, we will use the notation $Y_{a_i a_j}$ (resp., $X_{a_i a_j}$) to refer to the sum of the lengths of all the vertical (resp., horizontal) segments in $a_i, \ldots, a_j$.

By construction of P_x and the definition of the emanation graph, the length of any horizontal segment on P_x is at least as large as the subsequent vertical segment. Hence for every subpath $a_i, \ldots, a_j$ in P_x, which starts with a horizontal segment, we will have $X_{a_i a_j} \geq Y_{a_i a_j}$.

Without loss of generality assume that t lies on or above P_x. We now construct another path P_y following the same construction as that of P_x, but following the upward segments. Note that t is now in the region bounded by the paths P_x and P_y. We now construct an $(-x - y)$-monotone path P_t starting at t. P_t starts at t and follows the leftward segment. If the last segment ℓ of P_t is stopped by a horizontal (resp., vertical) segment ℓ', then we follow ℓ' towards the leftward (resp., downward) direction.

Note that P_t now either intersects P_x or P_y. Assume first that P_t intersects P_x at point q (see Figure 5). Let ℓ_h be the horizontal line through s. Assume that t lies above and q lies below ℓ_h (Note that the other cases would give rise to a smaller spanning ratio). Let r be the intersection point of P_t with ℓ_h. Thus the sum of the length of subpath of P_s from s to q and the subpath of P_t from q to t is as follows:

$$
\begin{aligned}
|sq|_x + Y_{sq} + |qt|_x + |qt|_y &= (|sq|_x + |qt|_x) + Y_{sq} + |qt|_y \\
&= |st|_x + Y_{sq} + |qt|_y \\
&= |st|_x + Y_{sq} + |qr|_y + |rt|_y \\
&\leq 2|st|_x + Y_{sq} + |rt|_y \\
&\leq 2|st|_x + |st|_x + |rt|_y \\
&= 3|st|_x + |rt|_y \\
&= 3|st|_x + |st|_y
\end{aligned}
$$

Therefore, the spanning ratio is: $f = \frac{(3|st|_x + |st|_y)}{\sqrt{(|st|_x)^2 + (|st|_y)^2}}$. To find and upper bound we need to maximize f, therefore we expect $|st|_x = 3|st|_y$, thus $f \leq \sqrt{10} \approx 3.162$.

Assume now that P_t intersects P_y at point q. But this case would be the same as when P_t intersects P_x with t lying on the upward cone of s. However, applying the same analysis, we again get an upper bound of $(3|st|_x + |st|_y)$ on the length of the path $s, \ldots, q, \ldots, t$, and hence an upper bound of 3.162. □

3.2 Generalization

Note that instead of grades, emanation graphs can also be defined with any set of r rays emanating from each vertex, where the rays create r cones of equal angle $\theta = 2\pi/r$. In this section, we prove a general upper bound on the spanning ratio of emanation graphs with r rays, where $r = 4q + 2$, where $q \geq 1$. We first describe the concept of angle-monotone paths.

A polygonal path is an *angle-monotone path of width* γ if the angles of any two edges in the path differ by at most γ (Figure 7(a)). Every angle-monotone path of width γ is a $(\frac{1}{\cos(\gamma/2)})$-spanner [3]. A geometric graph in the plane is angle-monotone of width γ if every pair of vertices is connected by an angle-monotone path of width γ. Hence these graphs are also $(\frac{1}{\cos(\gamma/2)})$-
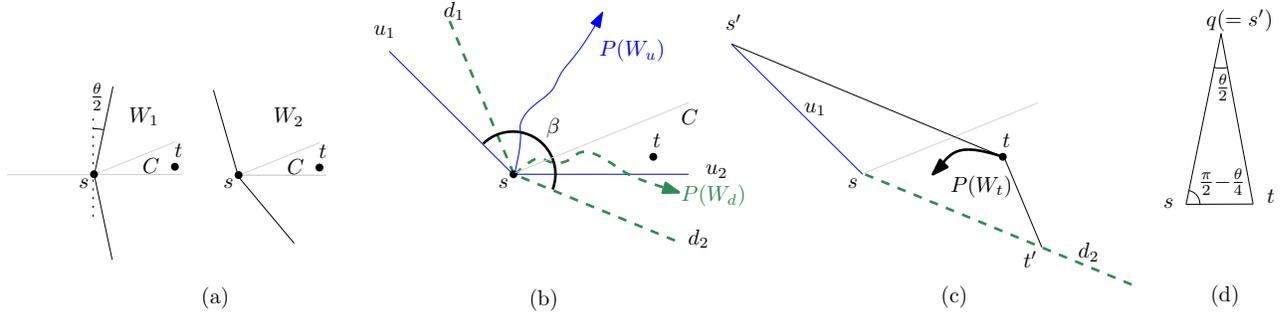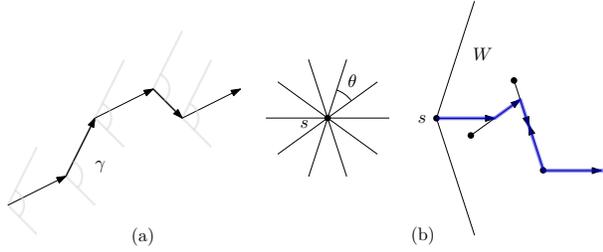
Figure 6: Illustration for the upper bound on the spanning ratio.

Figure 7: (a) An angle-monotone path of width γ. (b) Illustration for $P(W)$, where $r = 10$.

spanners. In the following we will prove that every emanation graph with r rays is an angle-monotone graph of width $\frac{1}{\sin(\pi/r)\sin(\pi/2r)}$.

Let M be an emanation graph with r rays, and let s and t to be a pair of vertices in G. Since we assumed that $r = 4q+2$, we may assume that there two horizontal rays around s, but *no vertical rays*. Let C be the cone incident to the rightward ray of s (lying above the ray), and without loss of generality assume that t lies in C (Figure 6(a)).

Let W be a wedge with angle $(\pi - \theta)$ such that the rightward ray of s is the bisector b of W (Figure 7(b)). By $P(W)$ we denote a path that starts following the ray parallel to b and continues as follows: If a segment stops the last segment of the current path, then we follow the ray towards the direction which is monotone with respect to b. If we reach an original vertex, then we continue to follow the ray parallel to the bisector. Note that $P(W)$ is an angle monotone path of width $(\pi - \theta)$ and lies entirely inside W.

We now define wedges $W_1, W_2, \ldots$ around s, where W_1 coincides with W and the subsequent cones are obtained by rotating W counter clockwise by an angle of θ (Figure 6(a)). Let W_u and W_d be two wedges, each of angle $(\pi - \theta)$ and contains t. Furthermore, $P(W_u)$ contains t or lies above t, and similarly, $P(W_d)$ contains t or lies below t. Let u_1 and u_2 be sides of W_u that lie above and below t, respectively. Similarly, d_1 and d_2 be the sides of W_d that lie above and below t, respectively.

Case 1: We first consider the case when W_u and W_d exist and choose W_u and W_d such that they minimize the angle β between u_1 and d_2 (Figure 6(b)). Note that $\beta \leq \pi$. Otherwise, by construction, β has to be at least $(\pi + \theta)$, and hence the wedge W' determined by d_1 and u_2 will be at least $(\pi - \theta)$. In this case, we can improve the choice of W_u and W_d further by replacing one of them using W'.

Let W_t be a wedge of angle $(\pi - \theta)$ with apex at t forming a quadrangle $ss'tt'$, as illustrated in Figure 6(c). In fact, we will choose W_t such that $\min\{\angle ss't, \angle st't\}$ is maximized. Note that $P(W_t)$ must intersect either $P(W_u)$ or $P(W_d)$ at some point q. We now use the path $P' = (s, \ldots, q, \ldots, t)$ to compute an upper bound on the spanning ratio. Since $P(W_u)$ and $P(W_d)$ are angle monotone paths of width $(\pi - \theta)$, the length of P' is at most $\frac{d_E(s,q)+d_E(q,t)}{\cos(\pi/2-\theta/2)}$. This term is maximized when $\angle ss't$ is the smallest, i.e., when $\angle ss't = (\theta/2)$, and $d_E(s,q) = d_E(q,t)$ (see Figure 6(d)). In this case, $d_E(s,q)+d_E(q,t) = 2\cdot d_E(s,q) = \frac{d_E(s,t)}{\sin(\theta/4)}$. Consequently, the length of P' is at most

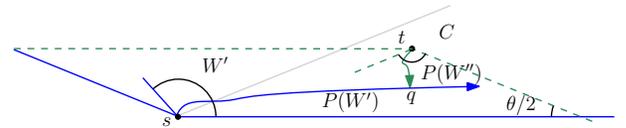$$\frac{d_E(s,q) + d_E(q,t)}{\cos(\pi/2 - \theta/2)} = \frac{d_E(s,t)}{\sin(\theta/2) \cdot \sin(\theta/4)}$$

Figure 8: Illustration for Case 2.

Case 2: The remaining case is when W_u and W_d do not exist. Without loss of generality assume that for every wedge W (with apex at s) of angle $(\pi - \theta)$ containing t, the path $P(W)$ lying below t. In this scenario, let W' be the wedge that contains C with one side determined by the rightward ray of s. We then consider a downward wedge W'' (with apex at t) of angle $(\pi - \theta)$, as illustrated in Figure 8. Let q be the intersection point of the paths $P(W)$ and $P(W'')$. Since $P(W)$ and $P(W'')$ are angle

monotone paths of width $(\pi - \theta)$, the spanning ratio in this case can be bounded to $(\frac{1}{\sin(\theta/2)\sin(\theta/4)})$ using the same analysis as in Case 1. The following theorem summarizes the result of this section.

Theorem 4 *The spanning ratio of every emanation graph with r rays, where $r = 4q + 2$ and $q \geq 1$, is at most $\frac{1}{\sin(\pi/r)\sin(\pi/2r)}$.*

4 Open Questions

For emanation graphs with 6 rays, Theorem 4 gives us an upper bound of 7.72, which is larger than the upper bound we obtained for the emanation graphs with four rays (i.e., M_1 has an upper bound of 3.16). This raises an interesting question of whether we can prove the lower bound on the spanning ratio of emanation graphs of grade 2 to be larger than 3.16. Note that such a scenario where increasing the number of cones increases the spanning ratio can be found in the context of Θ_r-graphs [5].

It would be interesting to find max-degree-4 planar geometric spanners with at most $4n$ Steiner points and a spanning ratio better than $\sqrt{10}$. Note that these bounds ($4n$ Steiner points, and spanning ratio $\sqrt{10}$) are currently achieved by emanation graphs of grade one (equivalently, by the competition mesh [18]).

References

[1] S. R. Arikati, D. Z. Chen, L. P. Chew, G. Das, M. H. M. Smid, and C. D. Zaroliagis. Planar spanners and approximate shortest path queries among obstacles in the plane. In *Algorithms - ESA '96, Fourth Annual European Symposium, Barcelona, Spain, September 25-27, 1996, Proceedings*, pages 514–528, 1996.

[2] L. Barba, P. Bose, M. Damian, R. Fagerberg, W. L. Keng, J. O'Rourke, A. van Renssen, P. Taslakian, S. Verdonschot, and G. Xia. New and improved spanning ratios for yao graphs. *Journal of Computational Geometry (JoCG)*, 6(2):19–53, 2015.

[3] N. Bonichon, P. Bose, P. Carmi, I. Kostitsyna, A. Lubiw, and S. Verdonschot. Gabriel triangulations and angle-monotone graphs: Local routing and recognition. In *Proceedings of the 24th International Symposium on Graph Drawing and Network Visualization (GD)*, pages 519–531, 2016.

[4] N. Bonichon, C. Gavoille, N. Hanusse, and L. Perkovic. Plane spanners of maximum degree six. In *Proceedings of the 37th International Colloquium, on Automata, Languages and Programming (ICALP)*, pages 19–30, 2010.

[5] P. Bose, J. D. Carufel, P. Morin, A. van Renssen, and S. Verdonschot. Towards tight bounds on theta-graphs: More is not always better. *Theor. Comput. Sci.*, 616:70–93, 2016.

[6] P. Bose, L. Devroye, M. Löffler, J. Snoeyink, and V. Verma. Almost all delaunay triangulations have stretch factor greater than pi/2. *Comput. Geom.*, 44(2):121–127, 2011.

[7] P. Bose, J. Gudmundsson, and M. H. M. Smid. Constructing plane spanners of bounded degree and low weight. *Algorithmica*, 42(3-4):249–264, 2005.

[8] P. Bose, D. Hill, and M. H. M. Smid. Improved spanning ratio for low degree plane spanners. *Algorithmica*, 80(3):935–976, 2018.

[9] P. Bose and M. H. M. Smid. On plane geometric spanners: A survey and open problems. *Comput. Geom.*, 46(7):818–830, 2013.

[10] L. P. Chew. There is a planar graph almost as good as the complete graph. In *Proceedings of the Third Annual Symposium on Computational Geometry (SoCG)*, pages 169–177, 1986.

[11] H. R. Dehkordi, F. Frati, and J. Gudmundsson. Increasing-chord graphs on point sets. *J. Graph Algorithms Appl.*, 19(2):761–778, 2015.

[12] D. P. Dobkin, S. J. Friedman, and K. J. Supowit. Delaunay graphs are almost as good as complete graphs. *Discrete & Computational Geometry*, 5:399–407, 1990.

[13] A. Dumitrescu and A. Ghosh. Lower bounds on the dilation of plane spanners. *Int. J. Comput. Geometry Appl.*, 26(2):89–110, 2016.

[14] D. Eppstein, M. T. Goodrich, E. Kim, and R. Tamstorf. Motorcycle graphs: Canonical quad mesh partitioning. *Comput. Graph. Forum*, 27(5):1477–1486, 2008.

[15] I. A. Kanj, L. Perkovic, and D. Türkoglu. Degree four plane spanners: Simpler and better. *Journal of Computational Geometry (JoCG)*, 8(2):3–31, 2017.

[16] J. M. Keil and C. A. Gutwin. Classes of graphs which approximate the complete euclidean graph. *Discrete & Computational Geometry*, 7:13–28, 1992.

[17] A. Lubiw and D. Mondal. Angle-monotone graphs: Construction and local routing. *CoRR*, abs/1801.06290, 2018.

[18] D. Mondal and L. Nachmanson. A new approach to GraphMaps, a system browsing large graphs as interactive maps. In *Proceedings of the 13th International Joint Conference on Computer Vision, Imaging and Computer Graphics Theory and Applications (VISIGRAPP)*, pages 108–119, 2018.

[19] L. Nachmanson, R. Prutkin, B. Lee, N. H. Riche, A. E. Holroyd, and X. Chen. GraphMaps: Browsing large graphs as interactive maps. In *Proceedings of the 23rd International Symposium on Graph Drawing and Network Visualization (GD)*, pages 3–15, 2015.

[20] G. Xia. The stretch factor of the delaunay triangulation is less than 1.998. *SIAM J. Comput.*, 42(4):1620–1659, 2013.

[21] G. Xia and L. Zhang. Toward the tight bound of the stretch factor of delaunay triangulations. In *Proceedings of the 23rd Annual Canadian Conference on Computational Geometry (CCCG)*, pages 175–180, 2011.

Appendix

Proof of Lemma 2

Proof. We use the construction described in Theorem 1 (e.g., see Figure 4) to show that any path from s to t is at least as large as the canonical path $\mathcal{L}$ (marked in blue). First observe that it suffices to restrict our attention to x-monotone paths. One can categorize the candidate monotone paths in two groups: (I) Paths that have the same length as $\mathcal{L}$, such paths can be formed by replacing segments of $\mathcal{L}$ by their symmetric counterparts, two of these counterparts are highlighted in yellow. (II) Paths with segments that do not belong to (I), two of such segments are highlighted in red. We only need to show that the paths in (II) can not be shorter than that of $\mathcal{L}$.

By the symmetric structure of the graph, it is straightforward to observe that the paths in (II) can gradually be transformed into the canonical path $\mathcal{L}$ without changing the length. For example, the yellow path from p_j to t can be replaced by the blue path from p_j to t. Here, we describe a proof by induction. In fact, we prove a stronger claim, i.e., $\mathcal{L}$ is a shortest path and for any original vertex q on the bottom guideline, a shortest path between s and q can be computed by following the rays closest to the guideline.

A formal way to see this is to apply an induction on the number of vertices. The claim is straightforward to verify when the emanation graph has only four vertices (e.g., consider the emanation graph determined by the rightmost four vertices in Figure 4). Assume now that the claim holds for the emanation graph of $2q$ vertices, where $4 \leq 2q < n(= 2q + 2)$, and consider the case when the graph has n vertices. Any x-monotone shortest path P of type (II) from s to t must pass through an original vertex other than s and t. If it passes through a vertex p_j on the bottom guideline, then the claim follows by induction. Specifically, we can choose p_j to be the source, and then the subpath p_j to t of P can be replaced by a subpath of $\mathcal{L}$ by induction. Note that the path from s to p_j can also be replaced by a subpath of $\mathcal{L}$ by induction. Thus $\mathcal{L}$ must be a shortest path between s to t.

On the other hand, if P passes through some vertex p_k on the top guideline, then we can swap the role of s and t to prove the existence of a path symmetric to $\mathcal{L}$ using the analysis used in the previous case. □